



W boson helicity measurement in $t\bar{t}$ dilepton channel at CDF

The CDF Collaboration
URL <http://www-cdf.fnal.gov>
(Dated: January 18, 2011)

We present the measurements of the fraction of longitudinally (f_0) and right-handed (f_+) polarized W bosons from top quark decay using $t\bar{t}$ events with the dilepton final state. W boson helicity fractions are determined by a comparison of angular distribution of leptons in W rest-frame ($\cos\theta^*$) with the templates corresponding to left-handed, right-handed and longitudinal fractions exclusively. Using CDF Run II data corresponding to integrated luminosity of 4.8 fb^{-1} , three measurements are performed. A model independent simultaneous measurement of f_0 and f_+ yields

$$\begin{aligned}f_0 &= 0.78_{-0.20}^{+0.19}(\text{stat.}) \pm 0.06(\text{syst.}) \\f_+ &= -0.12_{-0.10}^{+0.11}(\text{stat.}) \pm 0.04(\text{syst.})\end{aligned}$$

A measurement of f_0 constraining f_+ to its Standard Model value of 0.0 yields

$$f_0 = 0.62 \pm 0.11(\text{stat.}) \pm 0.06(\text{syst.})$$

while a measurement of f_+ constraining f_0 to its Standard Model value of 0.70 gives

$$f_+ = -0.07_{-0.05}^{+0.06}(\text{stat.}) \pm 0.03(\text{syst.})$$

All the results are consistent with Standard Model expectations.

Preliminary Results

I. INTRODUCTION

According to Standard Model (SM) the top quark decays very fast with the lifetime of about 5×10^{-25} s. Short lifetime prevents the hadronization of top quark, therefore its properties are transferred directly to decay products without modification caused by hadronization. Standard Model makes specific prediction about W boson polarization in case of $t \rightarrow Wb$ decay. Precise measurement of W polarization fractions could reveal new physics beyond the Standard Model.

Top quark decays to a W boson and b-quark with almost 100 % probability. W boson as a vector (spin 1) particle can have projections of spin on the direction of motion (helicity) $+1, 0, -1$, which are right-handed, longitudinal and left-handed helicity states, respectively. In the b-quark mass-less limit in the top quark decay and due to V-A nature of charge current weak interaction responsible for the decay, b-quark can be only left-handed and \bar{b} -quark (in \bar{t} decay) only right-handed. Top quark spin is $\frac{1}{2}$. Therefore the only option for W^+ (W^-) helicity state is left-handed (right-handed) and longitudinal in order to combine with left-handed b-quark to make combined spin projection $\pm 1/2$.

Different helicity states of W bosons are reflected in the angular distribution of the decay products. The differential decay rate for top quarks is given by:

$$\frac{1}{\Gamma} \frac{d\Gamma}{d\cos\theta^*} = f_- \cdot \frac{3}{8}(1 - \cos\theta^*)^2 + f_0 \cdot \frac{3}{4}(1 - \cos^2\theta^*) + f_+ \cdot \frac{3}{8}(1 + \cos\theta^*)^2 \quad (1)$$

where θ^* is the angle between momentum of the charged lepton (or down type quark) in the W rest frame and the momentum of the W boson in the top quark rest frame; f_- , f_0 and f_+ are the fractions for left-handed, longitudinal and right-handed helicity states, respectively and $f_- + f_0 + f_+ = 1$. The Standard Model gives specific prediction about fraction of cases when top quark decays into definite helicity states of W boson. At tree level, SM predicts for the longitudinal fraction f_0 :

$$f_0 = \frac{\Gamma(t \rightarrow W_0 b)}{\Gamma(t \rightarrow W_0 b) + \Gamma(t \rightarrow W_+ b) + \Gamma(t \rightarrow W_- b)} = \frac{M_t^2}{2M_W^2 + M_t^2} \quad (2)$$

In Standard Model $\Gamma(t \rightarrow W_+ b)$ is very close to zero ($f_+ = 3.6 \times 10^{-4}$) and SM predicts (at tree level) $f_0 = 0.703$, $f_- = 0.297$ for the top quark mass $175 \text{ GeV}/c^2$ [1].

In the beyond SM scenarios deviation from the SM expectation are possible due to presence of anomalous couplings [1].

The helicity fractions of the W boson from top quark decay has been measured by CDF and D0 collaborations in $t\bar{t}$ events [2]. It should be noted that almost all the measurements up to now (all simultaneous model independent measurements of f_0 and f_+) are statistically limited. The previous analyses were performed mostly in lepton+jets channel. The most precise analysis up to now have been performed by CDF in lepton+jet channel with the following results [3]: $f_0 = 0.88 \pm 0.11(stat) \pm 0.06(syst)$ and $f_+ = -0.15 \pm 0.07(stat) \pm 0.06(syst)$ for model independent simultaneous measurement while getting $f_0 = 0.70 \pm 0.07(stat) \pm 0.04(syst)$ (for fixed $f_+ = 0.0$) and $f_+ = -0.01 \pm 0.02(stat) \pm 0.05(syst)$ (for fixed $f_0 = 0.70$).

The existing analyses which used dilepton channel performed only model dependent determination of one fraction at a given time (D0 performed one analysis where dilepton channel have been used in combination with lepton+jets channel for simultaneous measurement of f_0 and f_+ [4]). Our measurement will be therefore a first model independent simultaneous measurement of W boson helicity fractions in dilepton channel only.

II. DATA SAMPLE & EVENT SELECTION

We use events with $t\bar{t}$ pair produced where both W's from top quark decay leptonically ($t\bar{t} \rightarrow W^+ b W^- \bar{b} \rightarrow \ell^+ \nu b \ell^- \bar{\nu} \bar{b}$).

The events under study produce two high- p_T leptons, missing transverse energy (\cancel{E}_T) from the undetected neutrinos, and the two jets coming from the hadronization of the b quarks. Additional jets are often produced by initial-state and final-state radiation.

This analysis is based on an integrated luminosity of 4.8 fb^{-1} collected with the CDF II detector between March 2002 and June 2009. We apply the event selection which have been used to measure the cross-section [5].

The data are collected with an inclusive lepton trigger that requires an electron or muon with $E_T > 18 \text{ GeV}$ [6]. From this inclusive lepton dataset, events with an offline reconstructed isolated electron or muon of $E_T > 20 \text{ GeV}$ are selected. A second electron or muon of E_T also greater than 20 GeV is also required using looser identification cuts and no requirement on isolation. Events with more than two leptons in the final state are rejected.

CDF II preliminary (4.8 fb⁻¹)

$t\bar{t}$ Signal Events with the tight SecVtx b-tag				
Source	ee	$\mu\mu$	$e\mu$	$\ell\ell$
WW	0.08±0.03	0.09±0.04	0.21±0.06	0.37±0.10
WZ	0.02±0.01	0.03±0.01	0.03±0.01	0.08±0.02
ZZ	0.08±0.06	0.07±0.06	0.02±0.02	0.17±0.14
DY+LF	0.51±0.05	0.60±0.05	0.28±0.03	1.39±0.12
DY+HF	0.51±0.04	1.41±0.11	0.37±0.03	2.28±0.18
Fakes	1.17±0.48	0.90±0.39	3.39±1.12	5.46±1.59
Total background	2.36±0.51	3.10±0.46	4.29±1.13	9.75±1.68
$t\bar{t}$ ($\sigma = 7.4$ pb)	30.22±1.91	29.63±1.87	70.10±4.38	129.96±8.10
Total SM expectation	32.59±2.32	32.73±2.25	74.39±5.42	139.71±9.66
Observed	22	44	71	137

TABLE I. The table shows the total number of background, SM signal expectation and data candidate events, The quoted uncertainties is the sum of the statistical and systematics uncertainty.

This "dilepton" dataset is cleaned of other known Standard Model sources with two leptons in the final state (dibosons, Drell-Yan events) by requiring missing transverse energy $\cancel{E}_T > 25$ GeV (or > 50 GeV if any lepton or jet is closer than 20° from the direction of MET) and high missing E_T significance for ee and $\mu\mu$ events with dilepton invariant mass in the Z peak. We also require the dilepton invariant mass to be larger than 5 GeV.

Additionally, we require at least 2 jets with $E_T > 15$ GeV identified in $|\eta| < 2.5$ (jet is defined as a fixed-cone cluster with a cone size of $R = 0.4$), scalar transverse energy sum $H_T > 200$ GeV and two leptons to be of opposite charge.

In order to have clean sample of $t\bar{t}$ events, we require that at least one of the reconstructed jets is identified as a jet coming from b-quark hadronization.

The number of events expected and also observed are presented in Tab. I. The kinematic distributions of the events passing above described event selection can be found in Fig. 1. There is good agreement between data and Monte-Carlo predictions.

III. METHOD

We use $\cos\theta^*$ distribution to determine W boson helicity fractions. Since the reconstructed $\cos\theta^*$ distribution is distorted from the theoretical one by many factors (selection, reconstruction, etc.), we use the template method. We get the estimate of W boson helicity fractions by comparing the $\cos\theta^*$ distribution from data to the simulated $\cos\theta^*$ distributions (templates) obtained for left-handed, longitudinal and right-handed W bosons respectively.

In order to reconstruct $\cos\theta^*$, the full $t\bar{t}$ kinematic chain has to be reconstructed. We use modification of the kinematic method previously applied for measurement of top quark mass [7]. It is briefly described below. After that, we will describe the template method used to determine the W helicity fractions themselves.

A. Kinematic reconstruction method

In dilepton channel we are dealing with an under-constrained system.

In each event, we are able to detect only charged leptons and jets coming from b-quarks. The two neutrinos are missing. However, there is partial information about escaped neutrinos and that is missing transverse energy (\cancel{E}_T), i.e. two components: $\cancel{E}_{Tx}, \cancel{E}_{Ty}$.

We assume a given value of top quark mass ($M_{top} = 175$ GeV) in order to be able to constrain the system and solve kinematic equations [8].

Because the measured quantities, i.e. momentum of the leptons, energy of the jets, and \cancel{E}_T have experimental uncertainties, this must be taken into account in the calculations. Therefore, we do smearing of jet energies and \cancel{E}_T (its \cancel{E}_{Tx} and \cancel{E}_{Ty} component), i.e. randomly generating (we do it 100 times) these quantities according to measured values within expected errors. Then, we try to find the solution by kinematic reconstruction of such smeared events.

In principal, there can be found up to 8 solutions. The four comes from kinematics (due to 2 undetected neutrinos), the other factor of two comes from two possible ways how to combine two leptons and two jets to form top and

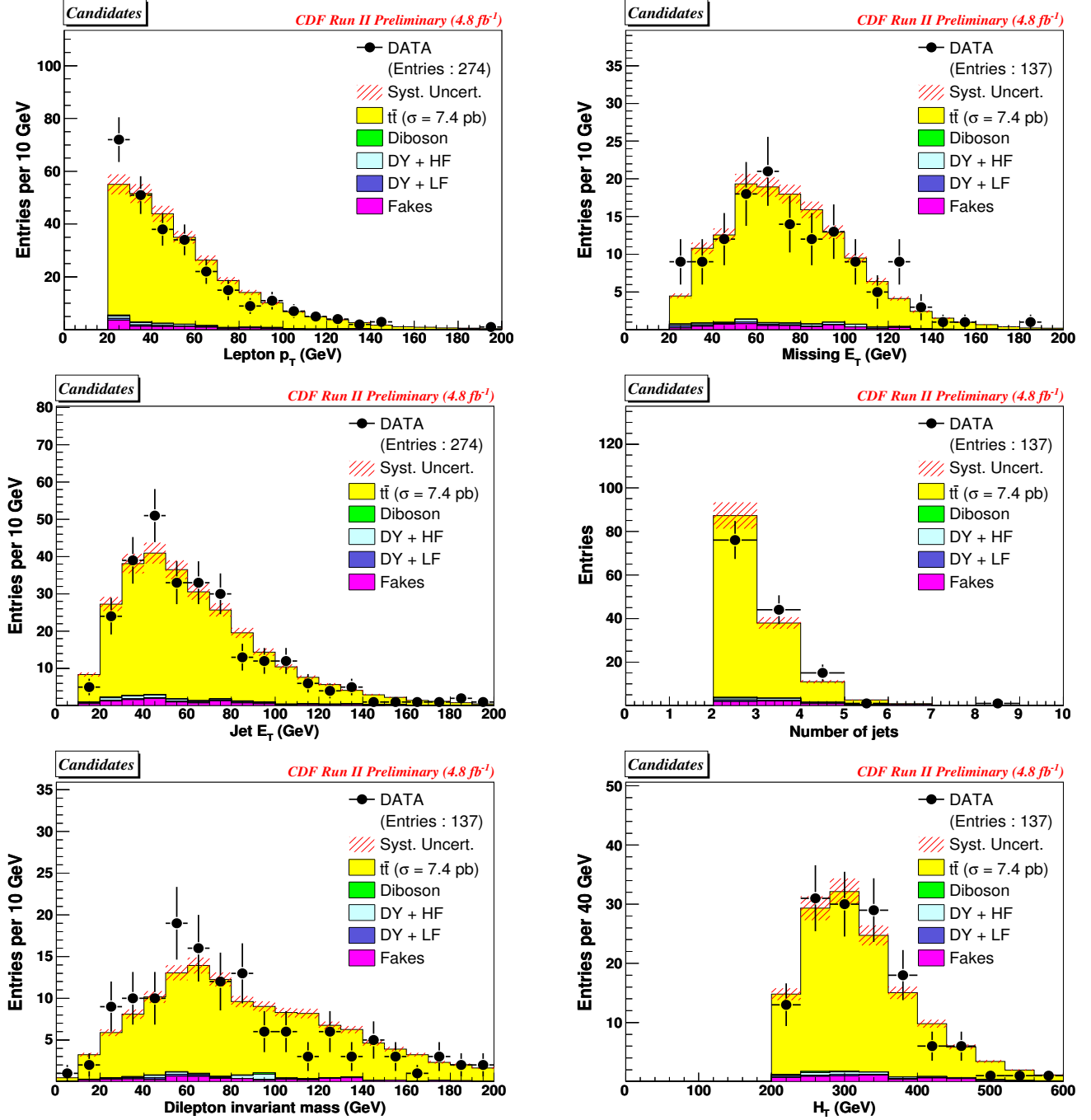


FIG. 1. Kinematic distributions for the events passing events selection.

anti-top (in case there are more than two jets we use just the two with highest E_T). We take just one of the 8 possible solutions according to the following criteria:

- from kinematically allowed solutions we take the one which has smallest effective mass of $t\bar{t}$ system,
- from two solutions allowed due to combination of leptons and jets, we take the one which has higher probability of reconstruction (in some topologies, it is not possible to find any of the 4 kinematically possible solutions), i.e. the combination which have more reconstructed “smeared” trials out of 100 trials for a given event.

B. $\cos \theta^*$ template method

Reconstructing $t\bar{t}$ kinematic chain (reconstructing four-vectors of top quark, W boson) using method described in the above section, we are able to reconstruct $\cos \theta^*$. Using $\cos \theta^*$ distribution, we determine W boson helicity fractions.

The reconstructed $\cos \theta^*$ distribution is shifted from the theoretically predicted distribution (Eq. 1) due to various reasons: selection will introduce some bias (e.g. requiring isolation on leptons cause the deficit of events with $\cos \theta^* \simeq -1.0$, requiring leptons to pass cut $p_T > 20$ GeV will also have impact because leptons from left-handed W bosons tend to have larger p_T than other leptons, etc.), reconstruction method can also cause some bias (e.g. in the events with more than 2 jets, there is possibility to use the jets from ISR/FSR instead of jets coming from b-quark hadronization, etc.). Therefore, we can not simply fit the resulting reconstructed $\cos \theta^*$ distribution by theoretical formula. The solution how to resolve this complication is to use the template method: create the templates for reconstructed $\cos \theta^*$ using Monte-Carlo simulated samples and then fit reconstructed $\cos \theta^*$ from data to these templates. As long as the procedure is applied consistently for the data and MC, the procedure should get an unbiased estimate of W boson helicity fractions even if reconstructed $\cos \theta^*$ distributions are shifted from the theoretical distributions.

1. $\cos \theta^*$ Templates for Signal and Background

We create signal templates using customized HERWIG (called 'GGWIG' [9]) high-statistics Monte Carlo samples. These samples contain exclusively left-handed, longitudinal and right-handed only W bosons, respectively. Figure 2 shows these templates together with simple polynomial fits.

The combined signal template f_s is given by the following formula

$$f^{sig}(\cos \theta, f_0, f_+) = \sum_{i=-,0,+} b_i * f_i^{sig} \quad (3)$$

$$b_i = \frac{\sum_{j=-,0,+} acc_{i,j} * f_i * f_j}{\sum_{i,j} acc_{i,j} * f_i * f_j}$$

where $f_- = 1 - f_0 - f_+$ and $acc_{i,j}$ is the acceptance for the case of one W having helicity 'i' and the other W in the same event have helicity 'j'.

This formula takes into account the fact that the acceptance is different for the events with different combination of helicities of W bosons from $t\bar{t}$ decays.

The dilepton channel has advantage of small background (see Tab. I) comparing to the other channels. The dominant backgrounds to dilepton $t\bar{t}$ events are diboson (WW, WZ, ZZ) production, Drell-Yan ($q\bar{q} \rightarrow Z/\gamma^* \rightarrow \ell^+ \ell^-$) production and mainly "fake" events where jet is falsely reconstructed as a lepton candidate (main source are $W \rightarrow \ell \nu + jet$ events)

Similarly as for the signal we create the templates also for the background samples. These backgrounds are then combined together according to the expected yield. Plot for the combined background template is in Fig. 2.

2. Likelihood fit

The final step in the determination of the W boson helicity fractions is the likelihood fit. We fit the $\cos \theta^*$ distribution of data candidates to the combination of signal and background templates.

We use a maximum likelihood method where the likelihood function has the following form:

$$\mathcal{L}(f_0, f_+, n_s, n_b) \equiv \mathcal{L}_{shape} \times \mathcal{L}_{Nev} \times \mathcal{L}_{bg} \quad (4)$$

$$\mathcal{L}_{shape} \equiv \prod_{i=1}^N \frac{n_s \times f^{sig}(\cos \theta_i^{rec}, f_0, f_+) + n_b \times f^{bckg}(\cos \theta_i^{rec})}{n_s + n_b}$$

$$\mathcal{L}_{Nev} \equiv \frac{e^{-(n_s+n_b)} (n_s + n_b)^N}{N!}$$

$$-\ln \mathcal{L}_{bg} \equiv \frac{(n_b - n_b^{exp})^2}{2\sigma_{n_b}^2},$$

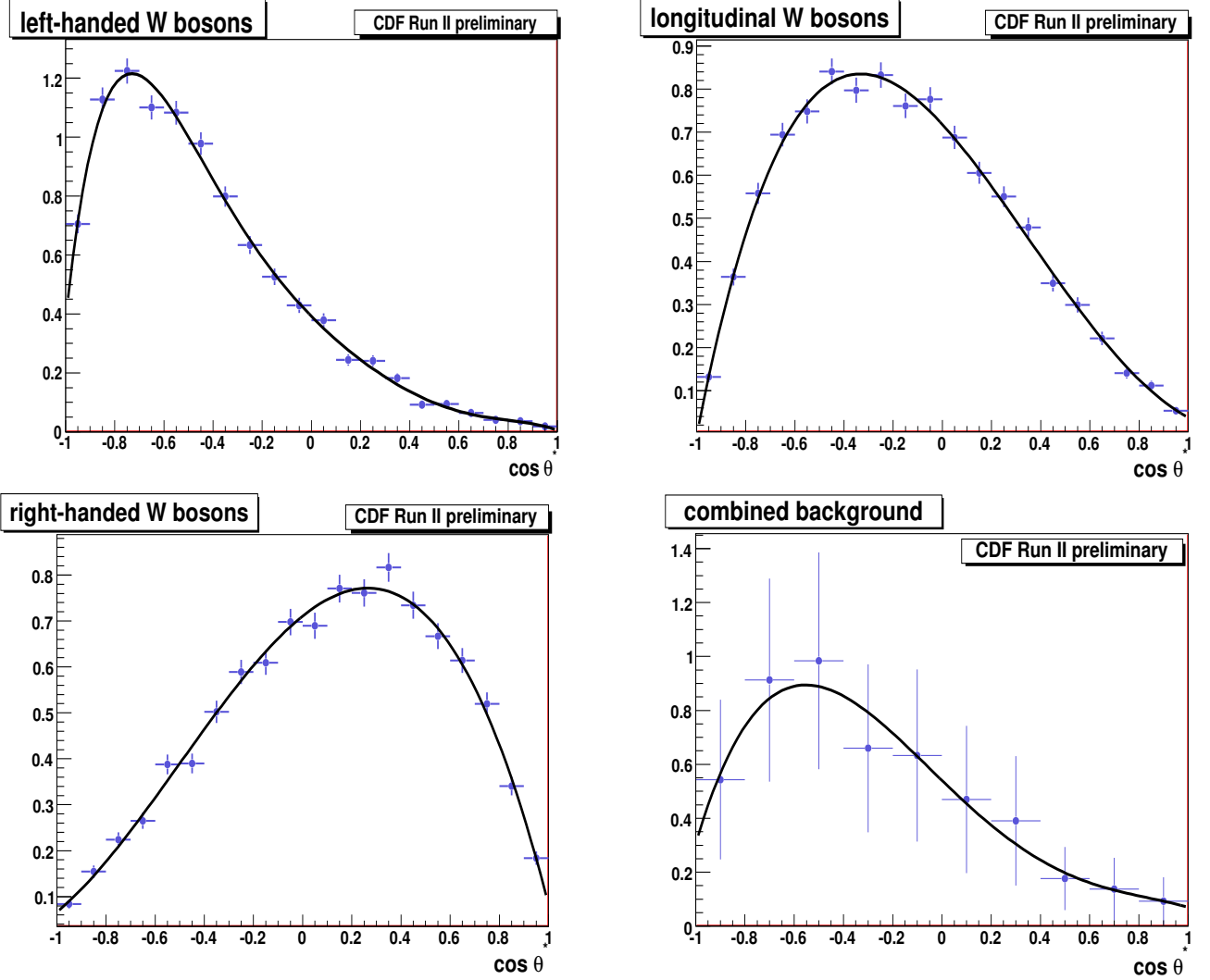


FIG. 2. The signal templates and combined background template.

where the number of background events is constrained by Gaussian in \mathcal{L}_{bg} and the Poisson term in \mathcal{L}_{Nev} makes sure the total number of events $n_s + n_b$ is in agreement with the N observed data events. The W boson longitudinal fraction (f_0), right-handed fraction (f_+), the number of background events n_b and the number of signal events n_s are free parameters in a likelihood function and are returned as a result of the fit.

IV. TESTING THE METHOD

Before we applied the reconstruction method on physics data, we checked it using Monte-Carlo simulated samples to prove that we are unbiased or in case we see the bias to derive a necessary correction. Also, we checked whether the method returns proper statistical uncertainty and how large uncertainty we should expect in data.

A. The individual measurements of f_0 and f_+

We perform the reconstruction for the full range of input f_0 (f_+) values while keeping the input value of f_+ (f_0) being equal to SM expected value -0.0 (0.7).

The dependence of reconstructed f_0 fraction on input f_0 fraction for fixed $f_+ = 0.0$ is shown in Fig. 3. Similarly, the dependence of f_+ (for input and fixed value of $f_0 = 0.7$) can be also seen in Fig. 3. The slope and the offset of

the dependencies are a slightly shifted from the expected values. We use the slope and offset of these dependencies to correct the results obtained in data.

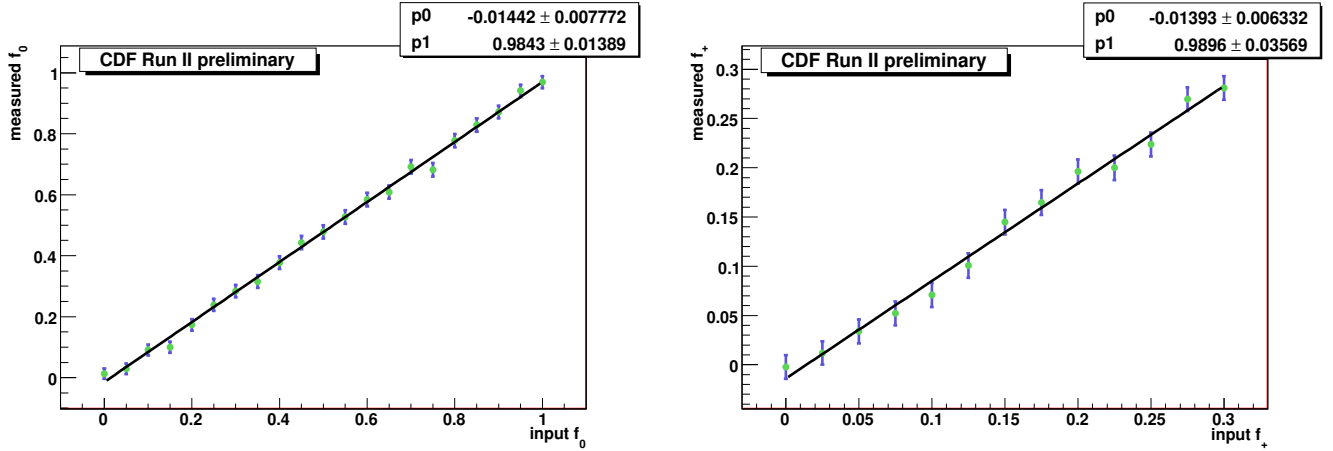


FIG. 3. The dependence of reconstructed f_0 fraction on input f_0 for fixed $f_+ = 0.0$ (left). The similar plot for f_+ dependence (fixed f_0) is shown on right.

We also performed the pseudo-experiments in order to check the reconstructed uncertainty of the helicity fraction.

We determine the expected uncertainty for f_0 to be 0.10 and for f_+ to be 0.05 by taking the mean value of uncertainty distribution from pseudo-experiments corresponding to the size of data sample.

B. The simultaneous model independent measurement of f_0 and f_+

We perform the test of simultaneous f_0 and f_+ reconstruction within full space of (f_0, f_+) input values.

For a given input value of f_+ (f_0) we perform the simultaneous fit of (f_0, f_+) and plot the dependence of reconstructed f_0 (f_+) on input value of f_0 (f_+). Fitting such dependence by straight line we get the slope and offset value of linear dependence for a given value of input f_+ (f_0). The dependencies of slope and offset of f_0 and f_+ linear dependence as a function of input f_+ and f_0 fraction are shown in Fig. 4 and Fig. 5, respectively. The slopes and the offsets are constant over large range of input values. Again, there is a little shift from expected values and we will use it to correct the results.

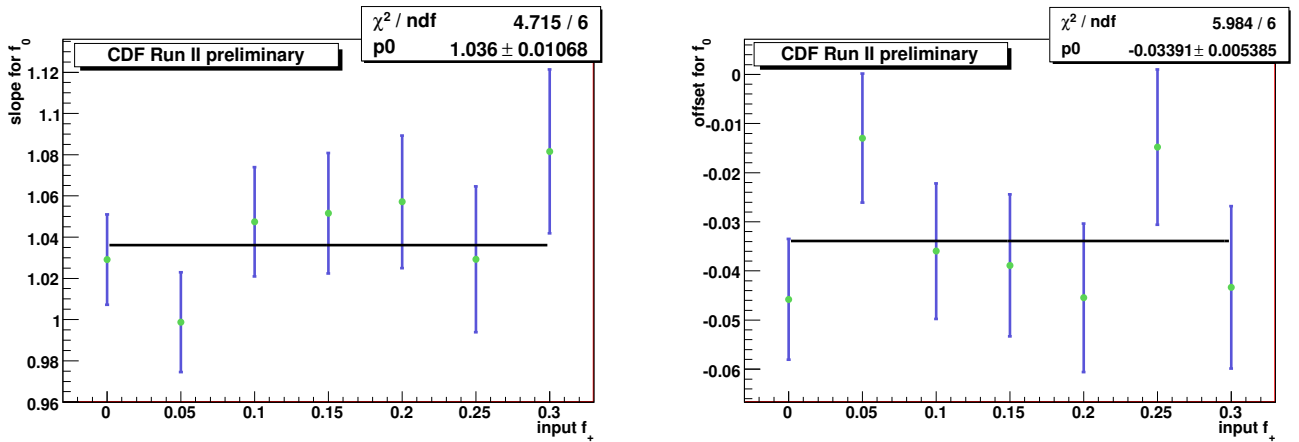


FIG. 4. The dependence of slope (left) and offset (right) for f_0 as a function of input f_0 .

Again, we perform the pseudo-experiments in order to check the reconstructed uncertainty.

We determine the expected uncertainty in the simultaneous fit to be 0.20 for f_0 and 0.11 for f_+ .

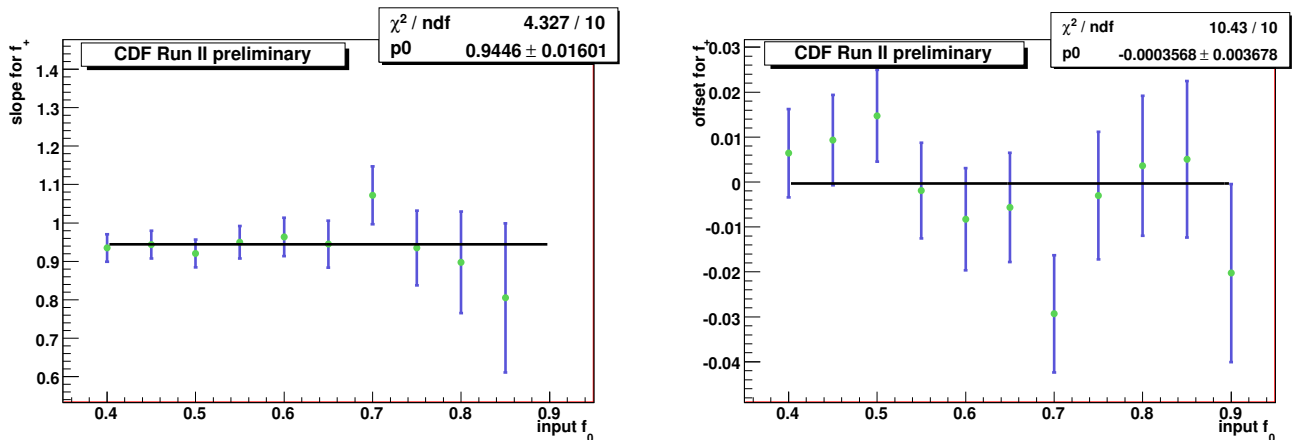


FIG. 5. The dependence of slope (left) and offset (right) for f_+ as a function of input f_+ .

V. SYSTEMATIC UNCERTAINTIES

The determination of W boson helicity fractions by our method is sensitive to the Monte Carlo simulated templates as well as to the jet reconstructions algorithms and different correction applied to them. We have performed studies in order to estimate the effect of each known source based on the pseudo-experiments MC studies. They are described below.

One of the largest sources of systematic uncertainty comes from the uncertainties on the jet energy corrections. We have studied it by changing the corrections by $\pm 1\sigma$.

Other source of systematics is due to different types of Monte Carlo generators. We compared the HERWIG [10] and the PYTHIA [11].

The initial and final state radiations (ISR and FSR) uncertainties are estimated using PYTHIA Monte Carlo samples in which QCD parameters for parton shower evolution are varied based on the studies of the CDF Drell-Yan data.

Another systematic error is coming from using different parton distribution functions (PDF). We have considered 20 pairs of CTEQ6 $\pm 1\sigma$ uncertainty sets, two sets of MRSTs for different Λ_{QCD} values, and the difference in CTEQ and MRST PDF groups.

We also evaluated the systematic error related to background. We estimated the uncertainty due to background shape by changing the individual backgrounds within their uncertainties in their amount while keeping the total amount of background fixed. The uncertainty in the total number of expected background events is taken into account in the likelihood fit (see Eq. 5).

We evaluate the effect of limited statistics of the signal and background templates by fluctuating the templates bin-by-bin and performing the measurement always using different templates.

We evaluate the effect of changing instantaneous luminosity over the period of CDF data taking by taking MC sample modeled with low (from early CDF runs) and high (using high inst. luminosity runs) luminosity profile.

The systematic uncertainties are summarized in Table II with the total systematic uncertainty of the measurement assumed to be independent sum of all partial systematic uncertainties due to different sources.

VI. DATA RESULTS

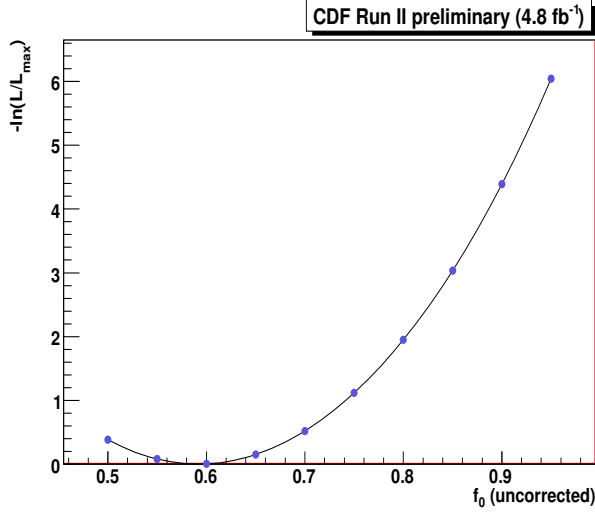
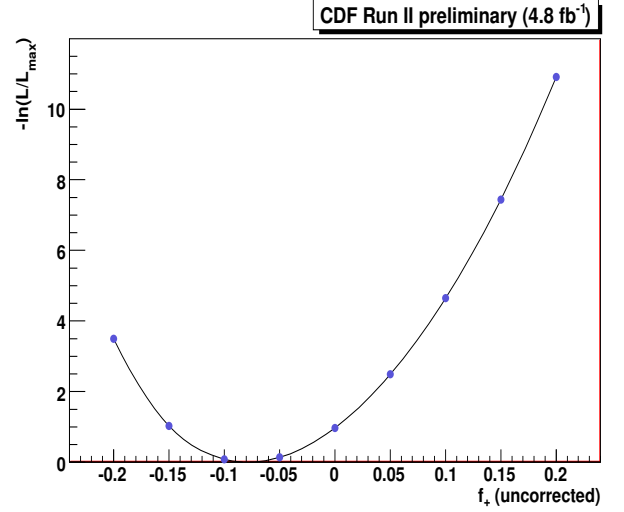
The same procedure which was extensively tested on Monte-Carlo simulated samples is applied to CDF data corresponding to integrated luminosity of 4.8 fb^{-1} . There are 137 events passing event selection. Out of these, 118 pass also the kinematic reconstruction.

We perform a measurement of f_0 fraction assuming SM expected value of $f_+ = 0.0$. The negative log-likelihood (NLL) profile corresponding to one dimensional f_0 fit can be seen in Fig. 6. The measured value of f_0 given by minimum of NLL is 0.59 ± 0.11 (stat.). Applying correction determined in Sec. IV A, we obtain the final estimate of f_0 : 0.62 ± 0.11 (stat.).

Next, we perform the fit of f_+ fraction while fixing f_0 to SM expected value $f_0 = 0.7$. The NLL corresponding to one dimensional f_+ fit can be seen in Fig. 7. The measured value of f_+ given by minimum of NLL is $-0.08^{+0.06}_{-0.05}$ (stat.).

CDF Run II preliminary (4.8 fb ⁻¹)				
Source	Δf_0 (f_+ fixed)	Δf_+ (f_0 fixed)	Δf_0 (model indep.)	Δf_+ (model indep.)
Jet Energy Scale	0.034	0.020	0.002	0.022
Generators	0.033	0.018	0.010	0.014
ISR/FSR	0.023	0.010	0.040	0.021
PDF	0.007	0.004	0.007	0.003
Background shape	0.007	0.005	0.006	0.008
Template statistics				
Signal	0.014	0.006	0.030	0.016
Background	0.009	0.004	0.021	0.012
Instant. luminosity	0.006	0.002	0.010	0.003
Total	0.056	0.031	0.056	0.041

TABLE II. Summary of systematic uncertainties.

FIG. 6. Negative log-likelihood profile of one-dimensional f_0 fit.FIG. 7. Negative log-likelihood profile of one-dimensional f_+ fit.

Applying correction determined in Sec. IV A, we obtain the final estimate of f_0 : $-0.07^{+0.06}_{-0.05}(stat.)$.

At the end, we perform model independent fit of both f_0 and f_+ fractions simultaneously. The NLL corresponding to simultaneous fit of both f_0 and f_+ can be seen in Fig. 8. The measured values of f_0 and f_+ given by minimum of NLL are $f_0 = 0.77^{+0.20}_{-0.21}(stat.)$ and $f_+ = -0.11^{+0.11}_{-0.10}(stat.)$. Applying correction determined in Sec. IV B, we obtain the final estimate of $f_0 = 0.78^{+0.19}_{-0.20}(stat.)$ and $f_+ = -0.12^{+0.11}_{-0.10}(stat.)$.

The comparison of $\cos \theta^*$ between data and simulation can be seen in Fig. 9.

A. Upper limit on f_+

Our measurement of f_+ is consistent with SM expectation of zero. By assuming SM value of $f_0 = 0.7$, we can determine the upper limit on f_+ .

We follow the Bayesian procedure, where we assume constant *a priori* probability density for f_+ within physically possible range $< 0.0, 0.3 >$. Multiplying the likelihood distribution by prior probability density, we arrive at a *posterior* probability density. The value of f_+ below which the area of posterior probability density is $\geq 95\%$ determines the upper limit on f_+ at 95 % C.L. When taking into account the systematic uncertainty by convoluting likelihood with Gaussian having mean zero and width equal to total systematic uncertainty of f_+ measurement, the upper limit on f_+ at 95 % C.L. is $f_+ < 0.09$, see Fig. 10.

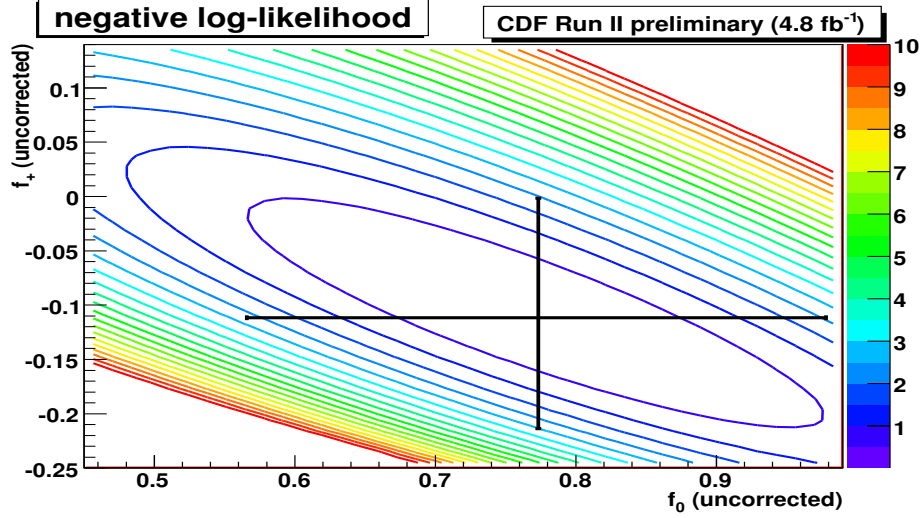


FIG. 8. Negative log-likelihood profile of two-dimensional simultaneous fit of both f_0 and f_+ .

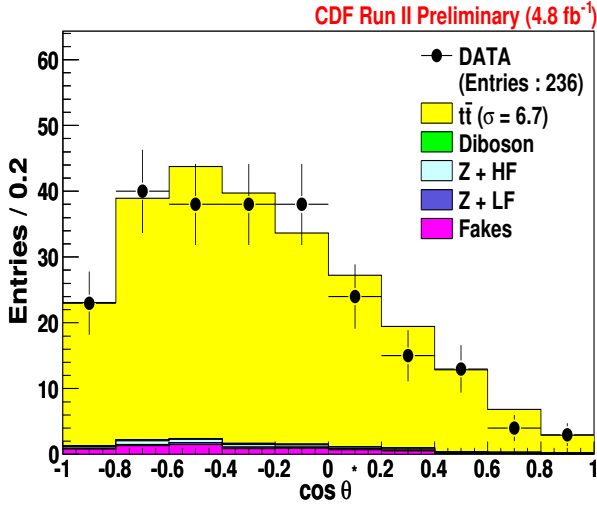


FIG. 9. $\cos \theta^*$ distribution comparison between data and expected signal and background

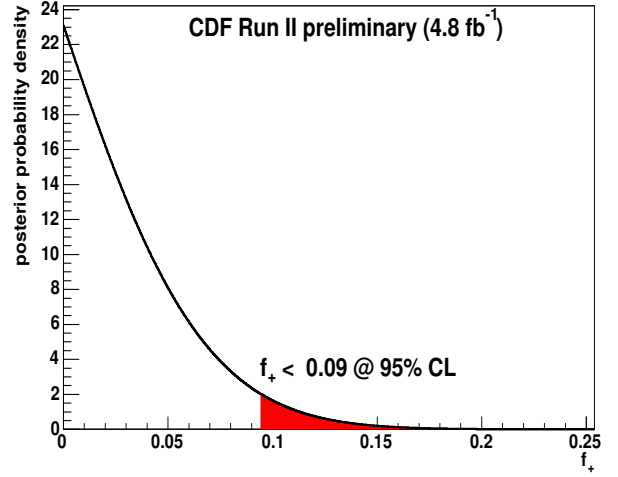


FIG. 10. The posterior probability density (with systematics included) as a function of right-handed W boson helicity fraction.

B. Top quark mass dependence

In our measurement, we assume top quark mass of $m_{top} = 175$ GeV. The fractions of W bosons with different helicity are function of m_{top} as can be seen from Eq. 2. Therefore, we estimate how the reconstructed fractions depend on m_{top} . The dependencies are shown in Fig. 11 for the case of the fit of one fraction while second fraction is fixed. The dependence for the case where both fractions are determined simultaneously is shown in Fig. 12.

VII. CONCLUSION

We have performed the measurement of W boson helicity fractions in top decays from $t\bar{t}$ dilepton events using 4.8 fb^{-1} of CDF data. The helicity fractions were determined by a comparison of angular distribution of leptons in W rest-frame ($\cos \theta^*$) between data and simulated templates.

Two kinds of measurements have been performed.

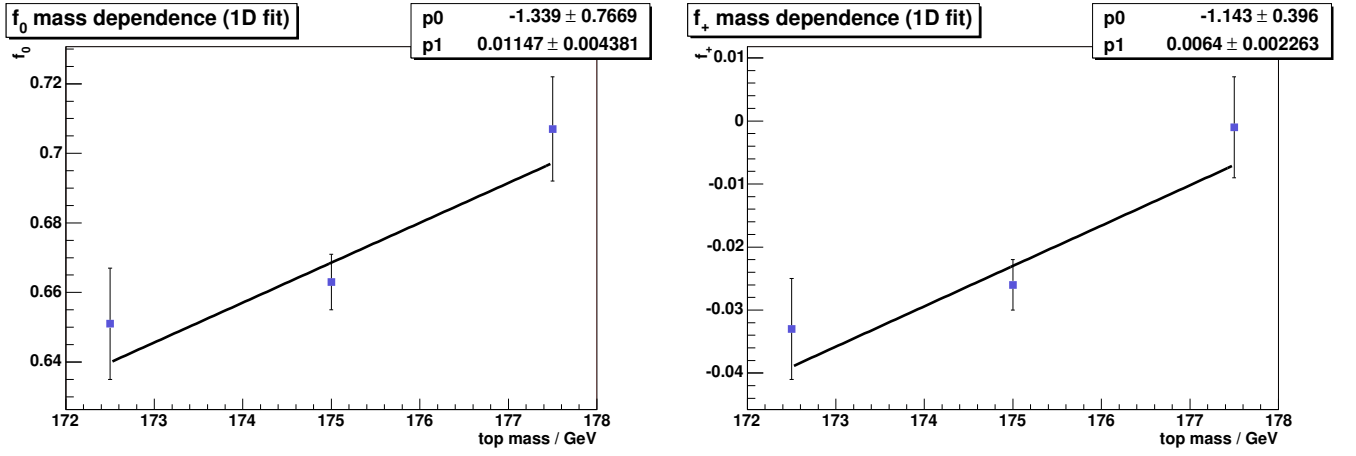


FIG. 11. The dependence of reconstructed f_0 (left) and f_+ (right) on top quark mass for the case of single fraction fit (second fraction is fixed).

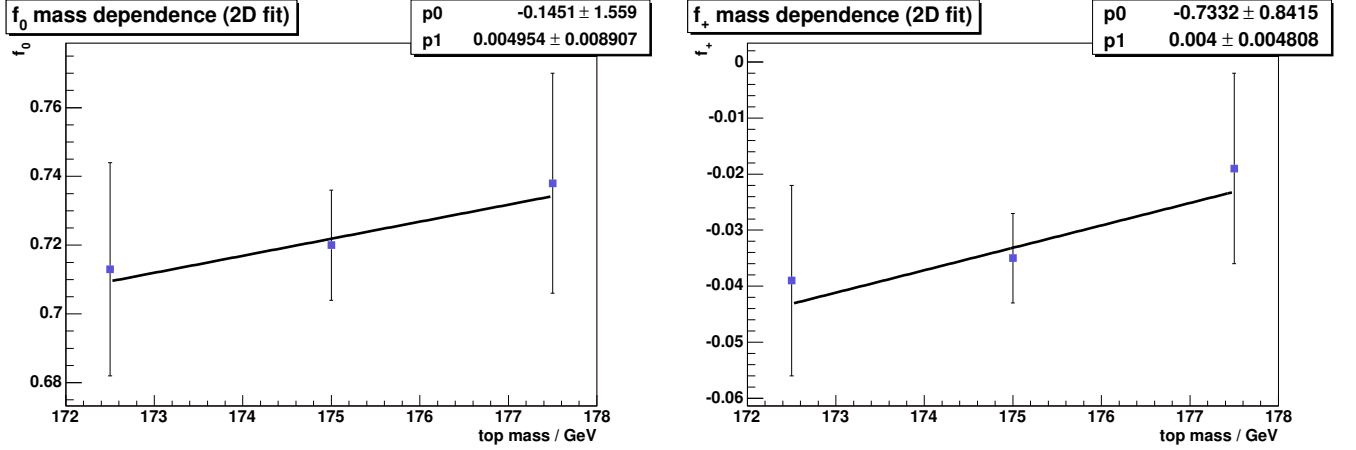


FIG. 12. The dependence of reconstructed f_0 (left) and f_+ (right) on top quark mass for the case of simultaneous fit of both f_0 and f_+ .

First, we assumed one fraction (f_0 , f_+ respectively) to have Standard Model expected value and determined the other fraction (f_+ , f_0 respectively). In such case, we measure f_0 to be (assuming $f_+ = 0.0$):

$$f_0 = 0.62 \pm 0.11(stat.) \pm 0.06(syst.)$$

and f_+ (assuming $f_0 = 0.7$):

$$f_+ = -0.07^{+0.06}_{-0.05}(stat.) \pm 0.03(syst.)$$

The model independent simultaneous measurement of f_0 and f_+ gives

$$f_0 = 0.78^{+0.19}_{-0.20}(stat.) \pm 0.06(syst.)$$

$$f_+ = -0.12^{+0.11}_{-0.10}(stat.) \pm 0.04(syst.)$$

All the results are consistent with Standard Model expectations. We expect that the precision of this measurement can be greatly improved by including (combining it with) the measurement using dilepton sample with no jet identified to originate from b-quark (there is expected gain of 110 signal and 100 background events in such sample). We plan to perform such measurement soon.

ACKNOWLEDGMENTS

We thank the Fermilab staff and the technical staffs of the participating institutions for their vital contributions. This work was supported by the U.S. Department of Energy and National Science Foundation; the Italian Istituto Nazionale di Fisica Nucleare; the Ministry of Education, Culture, Sports, Science and Technology of Japan; the Natural Sciences and Engineering Research Council of Canada; the National Science Council of the Republic of China; the Swiss National Science Foundation; the A.P. Sloan Foundation; the Bundesministerium für Bildung und Forschung, Germany; the World Class University Program, the National Research Foundation of Korea; the Science and Technology Facilities Council and the Royal Society, UK; the Institut National de Physique Nucleaire et Physique des Particules/CNRS; the Russian Foundation for Basic Research; the Ministerio de Ciencia e Innovación, and Programa Consolider-Ingenio 2010, Spain; the Slovak R&D Agency; and the Academy of Finland.

-
- [1] J. Aguilar-Saavedra *et al.*, Probing anomalous Wtb couplings in top pair decays, Eur. Phys. J. C50, 519 (2007); J. Cao *et al.*, Supersymmetric effects in top quark decay into polarized W boson, Phys. Rev. D68, 054019 (2003), F. del guila *et al.*, Precise determination of the Wtb couplings at the CERN Large Hadron Collider, Phys. Rev. D67, 014009 (2003), G. L. Kane *et al.* Using the top quark for testing standard-model polarization and CP prediction, Phys. Rev. D 45, 124 (1992)
 - [2] CDF collaboration, Phys. Rev. D73, 111103(R) (2006), CDF collaboration, Phys. Rev. Lett. 98 072001 (2007), D0 collaboration, Phys. Rev. Lett. 100, 062004 (2008), D0 collaboration, Phys. Rev. D72, 011104 (2005),
 - [3] CDF public note 10004
 - [4] D0 conference note 5722
 - [5] CDF public note 10163
 - [6] For the muons, transverse momentum P_T rather than transverse energy E_T is considered in the following text.
 - [7] A. Abulencia *et al.* [CDF Collaboration], “Measurement of the top quark mass using template methods on dilepton events in proton antiproton collisions at $\sqrt{s} = 1.96$ -TeV,” Phys. Rev. D **73**, 112006 (2006)
 - [8] Further, we make an assumption about the mass of the neutrinos ($m_{\nu_1} \simeq m_{\nu_2} \simeq 0$) and the mass of W bosons ($m_{W^\pm} \simeq 80.4$ GeV).
 - [9] E. Guillian, Top quark decay kinematics in fully reconstructed tt events in the e or $\mu + \cancel{E}_T + \geq 4$ jet decay channel, PhD thesis, University of Michigan, 1999.
 - [10] G. Corcella *et al.*, HERWIG 6: An Event Generator for Hadron Emission Reactions with Interfering Gluons (including supersymmetric processes), JHEP **01**, 10 (2001).
 - [11] T. Sjostrand *et al.*, High-Energy-Physics Event Generation with PYTHIA 6.1, Comput. Phys. Commun. **135**, 238 (2001).